ANNALS OF GEOPHYSICS. 61, 5, SE560, 2018; doi: 10.4401/ag-7837

"AN ANALYTIC STUDY OF FRICTIONAL EFFECT ON SLIP PULSES OF EARTHQUAKES"

Jeen-Hwa Wang[1,*]

[(1)] Institute of Earth Sciences, Academia Sinica, Nangang, Taipei, Taiwan

Article history
Receveid **June 26, 2018**; accepted **November 9, 2018.**
Subject classification:
Slip pulse; Rise time; Duration time; 1-D spring-slider model; Friction.

ABSTRACT

Seismological observations show the existence of slip pulses with $T_R/T_D<0.3$, where T_R and T_D are, respectively, the rise time at a site on a fault and the duration time of ruptures over the fault. An analytical study of generation of a slip pulse is made based on the continuous form of 1-D spring-slider model, with uniform fault strengths, in the presence of linear, slip-weakening (SW) friction: $f=1-u/\Delta$ (u=the displacement and Δ=the characteristic distance) or linear, velocity-weakening (VW) friction: $f=1-v/\upsilon$ (v=the velocity and υ=the characteristic velocity). Let ω_0 and t_r are, respectively, the predominant angular frequency of the system and the arrival time at a site and define $\gamma=(1-1/\Delta)^{1/2}$ and $\sigma=(1-1/4\upsilon^2)^{1/2}$. There are complementary solution (CS), and particular solution (PS) of the equation of motion. The *CS* shows a slip pulse under some ranges of model parameters for *SW* friction and for *VW* friction when $\upsilon>>1$; while the *CS* shows a crack-like rupture for *VW* friction when υ is not too large. For *SW* friction, T_R and T_R/T_D decrease when the slip pulse propagates in advance along the fault and when ω_0 and γ increase. T_R and T_R/T_D also depend on v_R (rupture velocity) and increasing L (fault length). For the *PS*, T_p/T_D is a good indication to show the existence of pulse-like oscillations at a site, because T_p (the predominant period of oscillations at a site) is slightly longer than T_R. Results show the existence of a pulse-like oscillation at a site for the two types of friction. A pulse-like oscillation is generated when $\Delta>1.6$ for *SW* friction and when $\upsilon>0.6$ for VW friction. T_p/T_D decreases with increasing Δ. For the two types of friction, T_o/T_D decreases when v_R and L increase.

1. INTRODUCTION

Heaton [1990] first found the existence of slip pulses of earthquakes. Let T_R and T_D be the rise time of displacement at a site on a fault and the duration time of ruptures over the entire fault, respectively. He observed $T_R<<T_D$ and non-uniform T_R over the fault plane. This exhibits the complexity of slip over fault plane during an earthquake. Several groups of researchers also observed slip pulses from natural earthquakes [Wald et al., 1991; Wald and Heaton, 1994; Nakayama and Takeo, 1997; Chen et al., 2001; Huang et al., 2001; Nielson and Madariaga, 2003; Lee et al., 2007; Galetzka et al., 2015].

Heaton [1990] interpreted the generation of slip pulse-likes using a self-healing assumption based on a crack model in the presence of velocity-weakening (VW) friction. He only considered a small strip which occurs immediately after the rupture front. Johnson [1990] discussed short T_R by combining forward propagating waves and backward arresting (or healing) waves from the borders. But, Day et al. [1998] claimed that it is not necessary to consider self-healing as a factor for earthquake dynamics.

The slip pulses have been investigated based on the crack models in the presence of friction [Andrews, 1976, 1985; Day, 1982; Papageorgiou and Aki, 1983; Boatwright, 1988; Andrews and Ben-Zion, 1996;

Beeler and Tullis, 1996; Cochard and Madariaga, 1996; Perrin et al., 1995; Zheng and Rice, 1998; Nielsen et al., 2000; Lapusta et al., 2000; Ben-Zion and Huang, 2002; Nielsen and Madariaga, 2003; Coker et al., 2005; Rice et al., 2005; Ampuero and Ben-Zion, 2008; Urata et al., 2008; Ando et al., 2010; Garagash, 2012]. Friction used by those authors includes VW friction, SW friction, velocity- and state-dependent friction, and thermal-pressurized friction. Results suggest that rupture modes are controlled by several factors, including friction laws, fault strengths, stress conditions on faults, energy and heat generated by faulting, scaling laws of faults, and spatial-temporal complexity of fault slip. In addition, some researchers considered geometrical heterogeneity of slip is a mechanism to stop earthquake rupture. Beroza and Mikumo [1996] suggested that the short T_R could yielded by pre-existing stress with heterogeneous fault strengths.

The slip pulses have also been studied by some authors [Wu and Chen, 1998; Chen and Wang, 2010; Elbanna and Heaton, 2012] based on the 1-D spring-slider model (abbreviated as the 1-D BK model hereafter) proposed by Burridge and Knopoff [1967]. From analytic studies by using SW friction, Wu and Chen [1998] claimed that SW friction can result in the self-healing slip pulse and the width of a pulse depends on v_R and friction strength. From numerical studies by using VW friction Chen and Wang [2010] found the propagation of slip pulses with $T_R/T_D<0.1$ along the model. Their simulation results are in agreement with Heaton's observations. Elbanna and Heaton [2012] pointed out the differences between the BK model and crack models. According to linear elastic fracture mechanics, slip pulses are seldom generated in the continuum models because slipping region inside of a fault cannot release applied stress without continuous slip while rupture is extending. On the other hand, in the BK model slip pulses can be produced due to the following reason. Each slider can completely release stress exerted by the leaf springs by going back to their equilibrium position even while rupture is extending. In other words, each slider does not transfer stress after their stoppage and information on the length of rupture does not feedback.

Laboratory experiments also provide significant information on generation of slip pulses. Coker et al. [2005] observed the existence of both pulse-like and crack-like ruptures under certain conditions. Lykotrafitis et al. [2006] observed the pulse-like shear ruptures with self-healing. Lu et al. [2007] found that the rupture modes depend on the level of fault pre-stress and VW friction is important for earthquake dynamics. Biegel et al. [2008] found that off-fault damage can affect the slip-pulse velocity.

As mentioned previously, in order to generate slip pulses some authors prefer to VW friction, while other favor SW friction. In this study, I will investigate the frictional effects on the generation of slip pulses using the continuous form of the 1-D BK model with linear SW friction or linear VW friction. Hence, it is significant to examine which friction (SW or VW friction) is more capable than the other for yielding slip pulses.

2. ONE-DIMENSIONAL SPRING-SLIDER MODEL

2.1 MODEL

Burridge and Knopoff [1967] proposed the 1-D BK model (see Figure 1), in which there are N sliders and springs. A slider with mass, m, is connected to its nearest two neighbors by a coil spring of stiffness, K_c. Of course, the two end sliders are only connected to the respective one nearest slider. A moving plate with a constant velocity, V_p, pulls each slider through a leaf spring of stiffness, K_l. Each slider rests in its equilibrium state at time t=0. The position of i-th slider (i=1, ..., N) is denoted by X_i, which is measured from its initial equilibrium position, along the horizontal axis represented by the coordinate y. Hence, X_i is in a function of y and t. Each slider is exerted by a frictional force between it and the moving plate. The frictional force is usually a function of displacement, X_i, and particle velocity, V_i ($=dX_i/dt$), of the slider and shown by the function $F_i(X_i;V_i)$, which has a static frictional force of $F_{si}=F_i(X_i;0)$ at rest. The equation of motion is

$$m(\partial^2 X_i/\partial t^2)=K_c(X_{i+1}-2X_i+X_{i-1})-K_l(X_i-V_p t)-F_i(X_i;V_i) \quad (1)$$

In Equation (1), there is an implicate parameter 'a' which is the space between two sliders in the equilibrium state. The ratio $\kappa=K_c/K_l$ has been defined by Wang [1995] to be the stiffness ratio of the system. This ratio represents the level of conservation of energy in the system. Larger κ is equivalent to stronger coupling be-

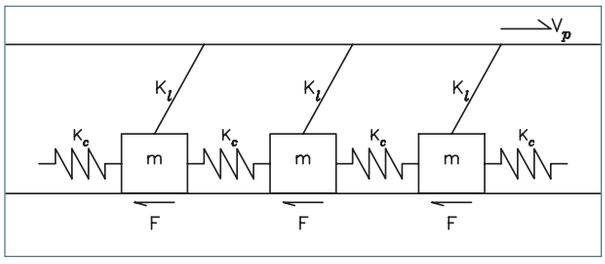

FIGURE 1. An N-degree-of-freedom dynamical spring-slider system.

tween two sliders than between a slider and the moving plate, thus leading to a smaller loss of energy through the leaf spring or a higher level of conservation of energy in the system, yet opposite for smaller κ. Since the fault system is dynamically coupling with dissipation, κ must be a non-zero finite value. The V_p is in the order of $\sim 10^{-12}$ m/s. The moving plate pulls a slider and thus gradually increases the elastic force, $K_c V_p t$, on it. When $K_c V_p t$ is slightly higher than static frictional force, Fsi, at the i-th slider, the two forces are cancelled out each other and can be ignored during ruptures. After a slider moves, F_{si} drops to F_{di} (i.e., the dynamic frictional force).

2.2 FRICTION

The frictional force between two contact planes is a very complicated physical process. Laboratory experiments have exhibited time-dependent static frictional strength of rocks [Dieterich, 1972] and velocity-dependent dynamic friction [Dieterich, 1979; Shimamoto, 1986]. Dieterich [1979] and Ruina [1983] proposed empirical, rate- and state-dependent friction laws. The detailed description of friction laws and the debates concerning the laws and their application to earthquake dynamics can be found in some articles [e.g., Marone, 1998; Wang, 2009; Bizzarri and Cocco, 2006a; Bizzari 2011].

Several simple friction laws have been taken to theoretically and numerically study earthquake dynamics [see Wang, 2016]. The laws are: the velocity-dependent, weakening-hardening friction law [Burridge and Knopoff, 1967]; the slip-dependent friction law [Cao and Aki, 1984/85]; the nonlinear VW friction law [Carlson and Langer, 1989a,b; Carlson, 1991; Carlson et al., 1991; and Beeler et al., 2008]; and the piece-wise, linear velocity-weakening and weakening-hardening friction [Wang, 1995, 1996]. Purely velocity-dependent friction could yield unphysical phenomena and mathematically ill-posed problems as pointed out by Madariaga and Cochard [1994]. Ohnaka [2003] stressed that the pure velocity-dependent friction law is not a one-valued function of velocity. The problem has been deeply discussed by Bizzarri [2011]. Nevertheless, for a purpose of comparison the single-valued linear velocity-dependent friction law is still considered below.

Friction is an important factor in controlling earthquake dynamics. Based on the 1-D BK model in the presence of linear VW friction with a decreasing rate, r_w, of friction force with velocity, Wang [1996] found three types of rupture propagation: (1) subsonic type with $r_w > 2(K_l m)^{1/2}$; (2) sonic type with $r_w = 2(K_l m)^{1/2}$; and (3) supersonic type with $r_w < 2(K_l m)^{1/2}$. Supersonic-type ruptures are non-causal, because v_R is greater than the sound speed. Knopoff et al. [1992] stated that the system is asymptotic to dispersive-free elasticity in the continuum limit when $r_w = 2(K_l m)^{1/2}$. They also found that large r_w is more capable of generating large events than small r_w. Carlson and Langer [1989a,b] used $F(v) = 1/(v+v_c)$ where v_c is the characteristic velocity. The related decreasing rate is $1/v_c(1+v/v_c)^2$ with the values in the range of from 1 to 0 when v_c varies from 0 to ∞. Hence, their friction law basically exhibits supersonic behavior with $r_w < 2(K_l m)^{1/2}$, and thus is potentially capable of producing very large events. Wang [1997] also stressed the effect of frictional healing on earthquake ruptures. Several authors [Nur, 1978; Carlson and Langer, 1989a,b; Carlson, 1991; Carlson et al., 1991; Knopoff et al.,1992; Rice, 1993; Wang and Hwang, 2001] stressed the influence on earthquake ruptures due to heterogeneous fault strengths on the fault. Carlson and her co-workers emphasized that de-localized events can be generated when the friction strengths over the fault plane is uniform.

In this study, I will analytically study the frictional effects caused by VW friction or SW friction on the generation of slip pulses by using the 1-D BK model. In order to perform analytic manipulation, only the linear laws are taken into account. The SW friction law (see Figure 2a) is:

$$F(X) = F_o(1 - X/X_c) \tag{2}$$

where X and X_c are, respectively, the displacement and the characteristic distance. The VW friction law (see Figure 2b) is:

$$F(V) = F_o(1 - V/V_c) \tag{3}$$

where $V = dX/dt$ is the velocity and V_c is the characteristic velocity. The breaking strengths are uniform over the model. This means that only steady travelling waves are taken into account.

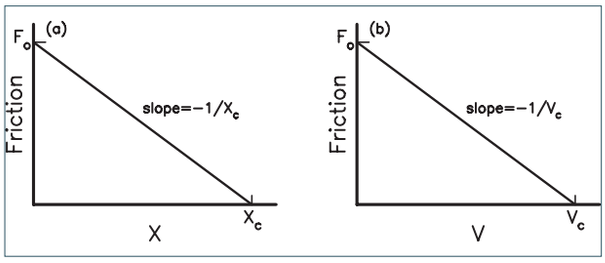

FIGURE 2. (a) For linear, slip-weakening friction law: $F(X) = 1 - X/X_c$ (X_c=characteristic displacement) and (b) for linear, velocity-weakening friction law: $F(V) = 1 - V/V_c$ (V_c =characteristic velocity).

4. ANALYTICAL MANIPULATION

4.1 EQUATION OF MOTION

Define $x_i=X_i-V_pt$. This gives $X_i=x_i+V_pt$ and $V_i=dX_i/dt=dx_i/dt+V_p=v_i+V_p$. Hence, Equation (1) becomes

$$m(\partial^2x_i/\partial t^2)=K_c(x_{i+1}-2x_i+x_{i-1})-K_lx_i-F_i(x_i+V_pt;v_i+V_p) \quad (4)$$

After a slider moves, V_pt and V_p can be neglected because of $V_pt<<x_i$ and $V_p<<v_i$ during ruptures. This makes Equation (4) be

$$m(\partial^2x_i/\partial t^2)=K_c(x_{i+1}-2x_i+x_{i-1})-K_lx_i-F_i(x_i;v_i) \quad (5)$$

Analytic manipulation will be performed based on the continuous form of Equation (5). The details how to set up the continuous form can be found in Carlson and Langer [1989a,b] and Wang [2016], and only a brief description is given below. Equation (5) is first normalized and then transformed to its continuous form. In order to normalize the equation, some normalization parameters must be defined below.

The natural angular frequency of oscillation of a single slider attached to a leaf spring in the absence of friction in Equation (1) is denoted by $\omega_0=(K_l/_m)^{1/2}$, and thus the related natural period is $T_0=2\pi/\omega_0$. Define $\tau=\omega_0t$ as the normalized time. Define $D_0=F_0/K_l$ as the characteristic slip distance of a slider exerted by a force F_0 through a spring with stiffness of K_l. Since the ratio D_0/V_p is the loading time for a leaf spring to stretch enough for overcoming F_0, $V_p/D_0\omega_0$ is the ratio of the slipping time $\omega_0^{-1}(=T_0/2\pi)$ to the loading time. $F_i(x_i;v_i)$ is represented by $F_0\phi(x_i;v_i)$. Substituting $u_i=x_i/D_0$, $v_i=du_i/dt=(du_i/dt)/D_0$, and related normalized (dimensionless) parameters [Wang, 2016] into Equation (5) and performing some mathematical manipulation lead to

$$\partial^2u/\partial\tau^2=h^2(\partial^2u/\partial\xi^2)-u-\varphi(u;v) \quad (6)$$

In Equation (6), h^2, u, and v are, respectively, the limiting values of κa^2, u_i, and v_i when 'a' approaches zero. Meanwhile, ξ is the normalized coordinate of y-axis which is the horizontal axis coordinate along the model, i.e., $\xi=y/D_0$. Wang [2016] discussed in details the trial solution of Equation (6), i.e., $u=-\phi(u;v)\approx$constant, when $\partial^2u/\partial\tau^2=0$ and $\partial^2u/\partial\xi^2=0$.

4.2 SOLUTIONS BASED ON SLIP-WEAKENING FRICTION

The normalized SW friction law from Equation (2) is $\phi(u)=1-u/\Delta$ where $\Delta=X_c/D_0$ is the dimensionless characteristic distance. Equation (6) becomes

$$\partial^2u/\partial\tau^2=h^2(\partial^2u/d\xi^2)-u-(1-u/\Delta) \quad (7)$$

Since $\phi(u)$ is negative and unreasonable when $u>\Delta$, Equation (7) can work only for $u<\Delta$. When the driving force reaches the static strength of the friction whose value is unit in Equation (7), stability at the slider is determined by the competition between the rate of friction $|\partial F^{strength}/\partial u|=1/\Delta$ and the rate of stress-relaxation between the slider and the leap spring $|\partial F^{stress}/\partial u|=|\partial[h^2(\partial^2u/d\xi^2)-u]/\partial u|=|h^2\partial(\partial^2u/d\xi^2)/\partial u-1|$ at $u=0$. With the condition $1-1/\Delta>|\partial[h^2(\partial^2u/d\xi^2)-u]/\partial u-1|$, we have $|\partial F^{strength}/\partial u|>|\partial F^{stress}/\partial u|$. This means that stable motions cannot exist, and is in contrast with the known source time function for dynamic ruptures where an initial acceleration phase should exist. This again makes Equation (7) work only when $u<\Delta$. Under SW regime, Equation (7) means that $\max\{x_p\}=D_0/\gamma^2=X_c/(\Delta-1)$. This means $\Delta>1$.

To solve Equation (7), the Laplace Transformation (LT, denoted by $\mathcal{L}$), which can be seen in numerous textbooks [e.g., Papoulis, 1962], is used to transform it to a different form. The LT of Equation (7) is

$$h^2\partial^2U/\partial\xi^2+(s^2+1-\Delta)U=1/s \quad (8)$$

The solution of U includes the complementary solution, U_c, and particular solution, U_p, that is, $U=U_c+U_p$. According to the method given in Johnson and Kiokemeister [1968], the solution of Equation (8) is

$$U(\xi,s)=C_1e^{-\psi\xi/h}+C_2e^{\psi\xi/h}-1/s\psi^2 \quad (9)$$

where $\psi=(s^2+1-\Delta^{-1})^{1/2}$.

There are two types of waves from Equation (9): The first one is the travelling wave represented by the first term along the $+\xi$ direction and the second one along the $-\xi$ direction in its right-handed-side, i.e., $U_c(\xi,s)=C_1e^{-\psi\xi/h}+C_2e^{\psi\xi/h}$. The second one is the oscillation at a site given by the third term, i.e., $U_p(\xi,s)=-1/s\psi^2$. The second term of the first type with $\xi<0$ can be rewritten as $e^{-\psi|\xi|/h}$. The Inverse Laplace Transformation (ILT, denoted by $\mathcal{L}^{-1}$) of $U_c(\xi,s)$ with $|\xi|/h>0$ is

$$u_c(\xi,\tau)=C\{1-\gamma(|\xi|/h)J_1[\gamma(\tau^2-(|\xi|/h)^2)^{1/2}]/[\tau^2-(|\xi|/h)^2]^{1/2}\}H(\tau-|\xi|/h) \quad (10)$$

where $C=C_1$ or C_2, $\gamma=(1-\Delta^{-1})^{1/2}$, $J_1[...]$ is the first-order Bessel function, and $H(\tau-|\xi|/h)$ is the unit step function *($H(z)=0$ as $z<0$ and $H(z)=1$ as $z\geq0$)* representing a travelling plane wave. Since $\tau=\omega_0t$ and $\xi=y/D_0$ are, respec-

tively, the normalized time and normalized rupture distance, $h=v_R/D_0\omega_0$ is the normalized rupture velocity. When the rupture propagates from 0 to ξ_L, which is the normalized rupture length and equal to L/D_0 (L=the rupture length), the normalized duration time is $\tau_D=\xi_L/h$, and thus the duration time is $T_D=\tau_D/\omega_0=\xi_L/\omega_0 h$, thus giving $T_D=\xi_L/\omega_0 h=(L/D_0)/\omega_0(v_R/D_0\omega_0)=L/v_R$.

Let t_r be the arrival time of the travelling wave at a site y, that is, $t_r=|y|/v_R$. Substituting $u_c(\xi,\tau)=x_c(y,t)/D_0$, $\xi=y/D_0$, $\tau=\omega_0 t$, and $t_r=|y|/v_R$ into Equation (10) gives

$$x_c(y,t)=CD_0\{1-(\gamma\omega_0 t_r)[\gamma\omega_0(t^2-t_r^2)^{1/2}]/ (t^2-t_r^2)^{1/2}\}H[\omega_0(t-t_r)] \quad (11)$$

Equation (11) shows a propagating wave which is usually represented by a function of the form $G(t-|y|/v_R)$, where $t'=t-|y|/v_R$ is known as the retarded time for situations where causality holds [e.g., Perrin et al., 1995; Nielsen et al., 2000]. The rise time, T_R, is measured from $t'=0$ or $t=t_r=|y|/v$ to larger $t'=t^*$ when the wave amplitude and the particle velocity reach their respective peak values. The quantities inside {...} multiplied by CD_0 of Equation (11) show the wave amplitude.

In order to further understand the properties of Equation (11), we only need to examine the function $S_s(y,t)=1-(\gamma\omega_0 t_r)J_1[\gamma\omega_0(t^2-t_r^2)^{1/2}]/(t^2-t_r^2)^{1/2}$. Define θ to be $\gamma\omega_0(t^2-t_r^2)^{1/2}$, and thus $S_s(y,t)$ can be represented by $1-(\gamma^2\omega_0 t_r)J_1(\theta)/\theta$. When $t=t_r$, $\theta=0$ and $J_1(\theta)=0$. This makes the value of $J_1(\theta)/\theta$ be indefinite. From the l'Hospital theorem [see Johnson and Kiokemeister, 1968], we have $lim_{\theta\to 0}[J_1(\theta)/\theta]=lim_{\theta\to 0}[dJ_1(\theta)/d\theta]=lim_{\theta\to 0}[J_0(\theta)-J_1(\theta)/\theta]$. According to the recurrence relation of Bessel functions [Abramowitz and Stegun, 1972]: $J_1(\theta)/\theta=[J_0(\theta)-J_2(\theta)]/2$, we have $lim_{\theta\to 0}[J_1(\theta)/\theta]=1/2$ because of $J_0(\theta)=1$ and $J_2\theta)=0$ when $\theta=0$. Hence, $x_c(y,0)=CD_0/2$ and $C=2x_c(y,0)/D_0$. The value of constant C depends on the initial value of $x_c(y,0)$. The waveform $x_c(y,0)$ appears before the main rupture and can behaves like the nucleation phase. From the observations, they are very small [Beroza and Ellsworth, 1996; Ellsworth and Beroza, 1995,1998; Mori and Kanamori, 1996; Wang, 2017]. This suggests $x_c(y,0)=CD_0/2<<1$, and thus C could be small. The first-order Bessel function $J_1(\theta)$ is positive, but vibrates and decreases with increasing θ, and $(t^2-t_r^2)^{-1/2}$ or θ^{-1} also decays fast with time when $t>t_r$.

From $T_R=t^*-t_r$, t^* is the time when $S_s(y,t)$ reaches its peak value. This time is commonly calculated from the necessary condition, i.e., $dS_s(y,t)/dt=0$. This can be obtained by taking $dS_s(y,t)/dt=[dS_s(\theta)/d\theta]d\theta/dt=0$. Since $d\theta/dt=\gamma\omega_0(t^2-t_r^2)^{-1/2}$ cannot be zero when $t>t_r$, we only need $dS_s(\theta)/d\theta=0$ or $d[J_1(\theta)/\theta]/d\theta=J_0(\theta)-J_1(\theta)/\theta=0$. The condition of $dS_s(\theta)/d\theta=0$ at $\theta^*=\gamma\omega_0(t^{*2}-t_r^2)^{-1/2}$ leads to the following equality: $J_0(\theta^*)-J_1(\theta^*)/\theta^*=0$. Actually, numerous values of θ^* can make this equality hold. Among them, the first value is *1.975* [Abramowitz and Stegun, 1972], thus giving $\gamma\omega_0(t^{*2}-t_r^2)^{1/2}=1.975$ and $t^*=(t_r^2+3.901/\gamma\omega_0)^{1/2}$. This makes T_R be $t^*-t_r=t_r\{[1+3.901/(\gamma\omega_0 t_r)^2]^{1/2}-1\}$. Figure 4 demonstrates the plots of T_R versus t_r for various values of γ, and ω_0: (a) for $\gamma=0.1$, *0.25*, *0.5*, and *1.0* (from top to bottom) when $\omega_0=1$ *Hz*; and (b) for $\omega_0=0.1$, *0.2*, *0.5*, *1.0*, and *2.0 Hz* (from top to bottom) when $\gamma=1$. Obviously, T_R decreases rapidly with increasing t_r, thus meaning that T_R decreases when the slip pulse propagates along the fault.

It is interesting to investigate the variation in $S_s(y,t^*)$ with $y=v_R t_r$. Inserting t^* into $S_s(y,t)$ leads to $S_s(y,t^*)=1-\gamma\omega_0 t_r J^1[\gamma\omega_0(t^{*2}-t_r^2)^{1/2}]/(t^{*2}-t_r^2)^{1/2}$. Hence, $S_s(y,t^*)=1-\gamma\omega_0 t_r J^1\{\gamma\omega_0[t_r^2+3.901(\gamma\omega_0)^{-2}-t_r^2]^{1/2}\}/[t_r^2+3.901(\gamma\omega_0)^{-2}-t_r^2]^{1/2}|$ due to $t^*=(t_r^2+3.901/\gamma^2\omega_0^2)^{1/2}$ as mentioned above. This gives $S_s(y,t^*)=1-(\gamma\omega_0)^2(|y|/v_R)J_1(1.975)/1.975$, where $3.9011/2=1.975$, and thus $S_s(y,t^*)=1-0.294(\gamma\omega_0)^2(|y|/v_R)$ because of $J_1(1.975)=0.5782$ [see Abramowitz and Stegun, 1972]. When $S_s(y,t^*)=0$, we have $0.293(\gamma\omega_0)2(|y|/v_R)=1$. This gives $|y|=y_c=3.413v_R/(\gamma\omega_0)^2$ and $t_c=y_c/v_R=3.413/(\gamma\omega_0)^2$, where t_c is t_r related to y_c. Clearly, the value of y_c (>0) is a function of v_R, γ, and ω_0. Hence, $S_s(y,t^*)$ changes from positive (when $|y|<y_c$ or $t_r<t_c$) to negative (when $|y|>y_c$ or $t_r>t_c$) by passing through zero (when $|y|=y_c$ or $t_r=t_c$).

Figure 3a displays an example of a normalized waveform $S_s(y,t)/S_{smax}$, where S_{smax} is the value of $S_s(y,t)$ at t^* as defined before in the figure, of the rupture wave having a propagation velocity of v_R=2 km/sec and the predominant angular frequency of ω_0=1 Hz at a position on the y-axis when the wave propagates with a travelling time $t_r=3.607$ sec under the action of slip-weakening friction force with γ=0.9. This plot shows a

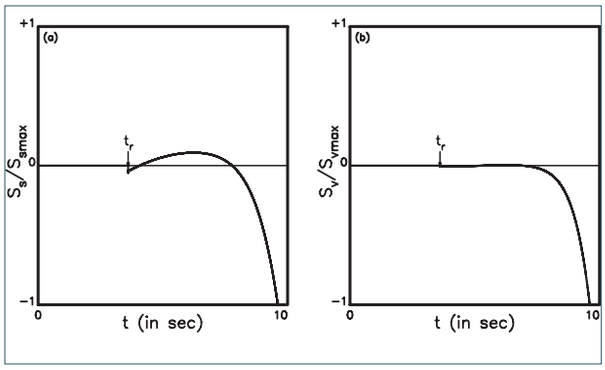

FIGURE 3. Figure shows $S_s(y,t)/S_{smax}$ ($S_{smax}=S_s(y,t^*)$) and $S_s(y,t)/S_{svmax}$ ($S_{svmax}=S_v(y,t^*)$) at $y=v_R t_r$ with v_R=2 km/sec and t_r=3.607 sec: (a) for $S_s(yy,t)/S_{smax}$ with γ=0.9 and ω_0=1.0 Hz; and (b) for $S_v(y,t)/S_{svmax}$ with σ=0.9 and ω_0=1.0 Hz.

pulse-like wave with short T_R. Since the value of t_c of this case is 4.216 sec, the related value of t^*, which is not displayed in Figure 3a, is positive as expected because of t_r=3.607 sec<t_c.

It is necessary to consider a quantitative criterion to confirm the existence of a slip pulse. A simple way is taken based on the value of T_R/T_D, which is

$$T_R/T_D=(v_R t_r/L)\{[1+3.901/(\gamma\omega_0 t_r)^2]^{1/2}-1\} \quad (12)$$

where $T_D=L/v_R$. In Equation (12), $v_R t_r$ (denoted by L_R) is the length along which the rupture has propagated on the fault. Obviously, T_R/T_D increases with L_R/L and decreases with increasing γ, or ω_0, or t_r. From the measures made by Heaton [1990], T_R/T_D is almost between 0.1 and 0.3. Chen and Wang [2010] gave T_R/T_D<0.1 from numerical simulations. Here, I assume that an acceptable quantitative criterion is T_R/T_D<0.3. Since, L_R/L is always less than 1 during earthquake ruptures, the request of T_R/T_D<0.3 will be mainly dependent on γ, ω_0, and t_r. Nevertheless, it is easier to generate a slip pulse for long L than for short L.

The inequality T_R/T_D<0.3 can be represented by $[1+3.901/(\gamma\omega_0 t_r)^2]^{1/2}$<1.3. When the rupture proceeds, t_r always increases and makes the inequality hold. Hence, t_r is less important on the inequality especially for t_r>1 sec, which appears very soon after an earthquake starts to rupture. Since the slip pulses have frequencies in a small range of 0.5 to 2 Hz, ω_0 is not the main factor. Since the value of γ varies in a large range from 0^+ to 1, γ must be the main factor in controlling the slip pulse. Considering an example of a slip pulse with ω_0=1 Hz and γ=1, we have $(1+3.901/t_r^2)^{1/2}$<1.3. When t_r>2.378 sec, the inequality T_R/T_D<0.3 always holds and thus the slip pulse appears. Figure 6 displays the plots of t_r versus γ for ω_0=0.1, 0.2, 0.5, 1.0, and 2.0 Hz (from top to bottom). The area between the curve and vertical line denotes the solution regime. Clearly, t_r decreases with increasing ω_0. The example shown in Figure 3a can meet the condition. Figure 5 displays the plots of T_R/T_D versus t_r with v_R=2 km/sec for various values of γ, ω_0, and L: (a) for γ=0.1, 0.25, 0.5, and 1.0 (from top to bottom) when L=50 km and ω_0=1 Hz; (b) for ω_0=0.1, 0.2, 0.5, 1.0, and 2.0 Hz (from top to bottom) when L=50 km and γ=1; and (c) for L=10, 30, 50, 70, 100 km (from top to bottom) when γ=1 and ω_0=1 Hz. Obviously, T_R/T_D decreases very rapidly with increasing t_r, thus meaning that T_R decreases when the slip pulse propagates along the fault. Meanwhile, T_R also decreases when γ, ω_0, and L increase.

The third term of Equation (9), i.e., $U_p(\xi,s)=-1/s(s^2+1-\Delta^{-1})$, is not a function of locality and thus only represents the oscillations at all sites on the fault. But, it is still significant to examine if it behaves like a pulse-like oscillation or not. Its ILT is $u_p(\xi,\tau)=\mathcal{L}^{-1}[U_p(\xi,s)]=[1-\cos(\gamma\tau)]/2\gamma$. The solution exists when Δ>1. For Δ>1, we have

$$u_p(\xi,\tau)=[1-\cos(\gamma\tau)]/2\gamma=\sin^2(\gamma\tau/2)/\gamma^2 \quad (13)$$

The particular solution $u_p(\xi,\tau)$ comes from the ILT of $-1/s(s^2+1-\Delta^{-1})$. Equation (8) leads to $h^2\partial^2U/\partial\xi^2=-(s^2+1-\Delta^{-1})U+1/s$, in which $-(s^2+1-\Delta^{-1})U$ behaves like the LT of an elastic force and $1/s$ is the LT of 1 (see Equation (8)) normalized from the static friction force, F_0. When $h^2\partial^2U/\partial\xi^2$=0, i.e., the divergence of U along the ξ-axis is zero, we have $(s^2+1-\Delta^{-1})U=1/s$. This indicates a bal-

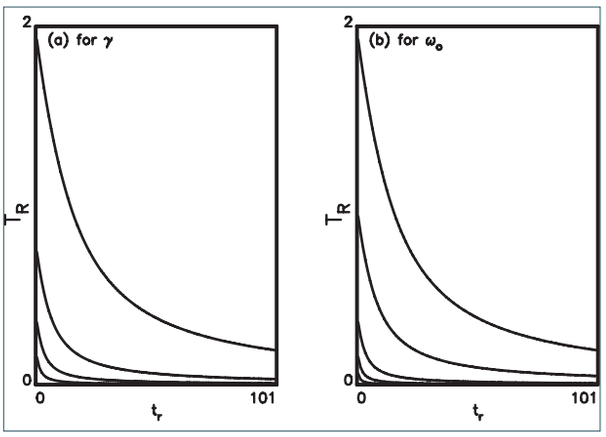

FIGURE 4. The plots of T_R versus tr for various values of γ and ω_0: (a) for γ=0.1, 0.25, 0.5, 1.0, and 2.0 (from bottom to top) when ω_0=1 Hz; and (c) for ω_0=0.1, 0.2, 0.5, 1.0, and 2.0 Hz (from bottom to top) when γ=1.

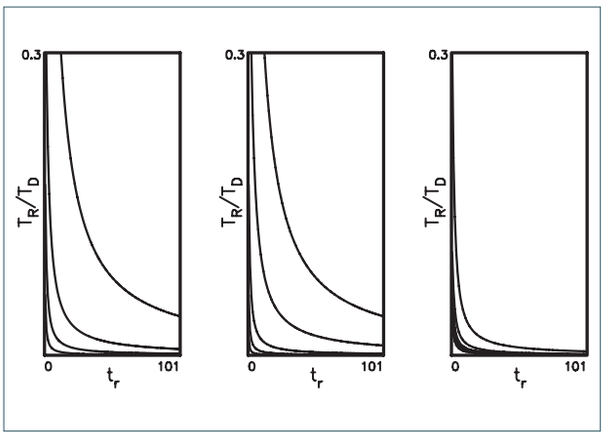

FIGURE 5. The plots of T_R/T_D versus tr for various values of γ, ω_0, and L: (a) for γ=0.1, 0.25, 0.5, and 1.0 (from top to bottom) when L=50 km and ω_0=1 Hz; (b) for ω_0=0.1, 0.2, 0.5, 1.0, and 2.0 Hz (from top to bottom) when L=50 km and γ=1; and (c) for L=10, 30, 50, 70 km.

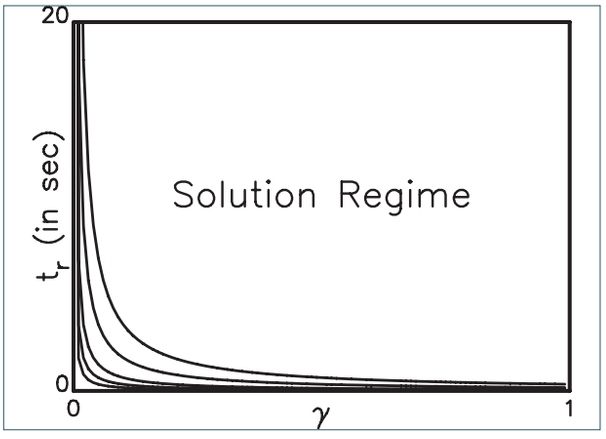

FIGURE 6. The plots of tr versus γ for ω_0=0.1, 0.2, 0.5, 1.0 and 2.0 Hz (from top to bottom) based on SW friction.

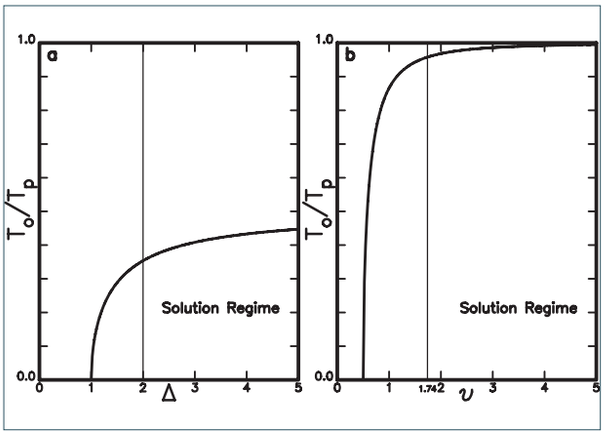

FIGURE 7. (a) The plots of T_0/T_p versus Δ; and (b) the plots of T_0/T_p versus υ for SW friction. The vertical line shows the value of Δ or υ at which the curve becomes flat.

ance between the elastic force and the static friction force and its ILT shows a vibration on the fault. The two forces behave like pre-existing forces on the fault plane. Since the two forces are of locality- independence, the related particular solution is also of locality-independence. Inserting Equation (13) into Equation (7) results in $\partial^2 U/\partial\tau^2=-(1-\Delta^{-1})u_p-1$. Since the initial value of u_p is zero, we have $\partial^2 u/\partial\tau^2=-1$, thus implying a negative initial acceleration at a slider. There are two cases in Equation (13): one with $1-\Delta^{-1}<0$ or $\Delta<1$ and the other with $1-\Delta^{-1}>0$ or $\Delta>1$. The first case is $sin[(1-\Delta^{-1})^{1/2}\tau/2]= i\, sinh[(\Delta^{-1}-1)^{1/2}\tau/2]$, and thus $sin^2[(1-\Delta^{-1})^{1/2}\tau/2]=-sinh^2[(\Delta^{-1}-1)^{1/2}\tau/2]$. This solution exhibits a negative hyperbolic sine-type function, which cannot be a common wave, and can be ignored. The second case represents a positive sine-type function and thus can represent a vibration at all sites because it is site-independent from Equation (13). Replacing $u_p(\xi,\tau)$ by $x_p(y,t)$ and τ by $\omega_0\tau$ into Equation (13) leads to

$$x_p(x,t)=D_0 sin^2(\gamma\omega_0 t/2)/\gamma^2 \qquad (14)$$

Define $\omega^*=\gamma\omega_0/2=(1-\Delta^{-1})^{1/2}\omega_0/2$ to be the predominant angular frequency of the oscillation, and thus $T_p=2\pi/\omega^*$ is its predominant period. This gives $T_0/T_p=2/(1-\Delta^{-1})^{1/2}$. The plot of T_0/T_p versus Δ is shown in Figure 7a. T_0/T_p increases with Δ. The increasing rate of T_0/T_p with Δ is high when $\Delta<2$ and becomes low when $\Delta>2$.

Figure 8 shows the typical velocity waveform (in the solid plus dotted curve) and the typical displacement waveform (in the solid curve). Since the wave propagates from $-y$ to $+y$, it stops at the time instant when v=0. In Figure 8, T_p is the period of velocity waveform. Since $T_R\approx T_p/2$, the ratio of T_p over T_D, i.e., T_p/T_D, is a good indication to show whether a slip pulse can exist or not. The ratio T_p/T_D is $2T_0(1-\Delta^{-1})^{-1/2}/(L/v_R)=2(1-\Delta^{-1})^{-1/2}v_R T_0/L$, where $v_R T_0$ denotes a characteristic distance of wave propagation in the natural period. For real $M\geq 6$ earthquakes v_R varies from 1.5 to 4 km/s, L from 30 to 300 km, and T_0 from 10^{-1} to 10 sec. Figure 9 shows the plots of T_p/T_D versus Δ: (a) for $v_R T_0$=0.5, 1.0, 1.5, 2.0, 2.5, 3.0, 3.5, and 4.0 km (from bottom to top) when $\omega_0 L=80$ km/s; and (b) for $L=20$, 40, 60, 80, 100, 120, 140, and 160 km (from top to bottom) when $v_R T_0=2$ km.

As mentioned above, the quantitative criterion to confirm the existence of a slip pulse is $T_R/T_D<0.3$. Now, T_R is almost equal to T_p. Hence, a pulse-like oscillation can exist when $T_p/T_D<0.3$. In Figure 9, the upper bound of T_p/T_D is 0.3. Meanwhile, the solution

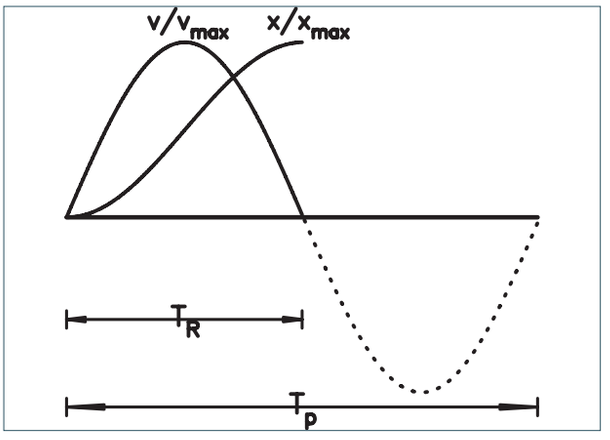

FIGURE 8. The solid plus dotted curve represents the velocity waveform and the solid curve denotes the displacement waveform. T_p and T_R are, respectively, the predominant period of the velocity waveform and the rise time of displacement waveform.

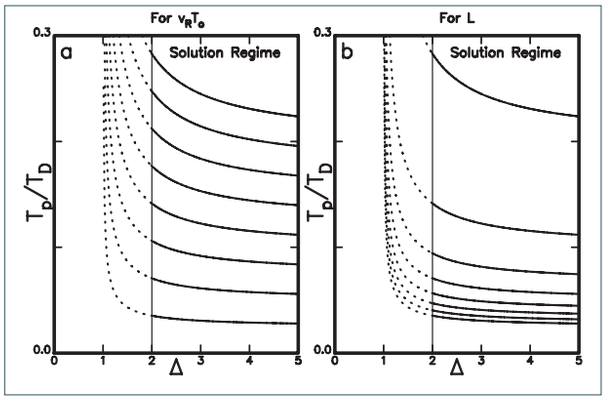

FIGURE 9. The plots of T_p/T_D versus Δ: (a) for v_RT_0=0.5, 1.0, 1.5, 2.0, 2.5, 3.0, 3.5, and 4.0 km (from bottom to top) when $\omega_0 L$=80 km/s; and (b) for L=20, 40, 60, 80, 100, 120, 140, and 160 km (from top to bottom) when v_RT_0=2 km.

exists only when Δ>2 (as displayed by a vertical line in the figure). Obviously, the major portion of each curve is below the upper bound, thus suggesting the existence of a pulse-like oscillation in the solution regime.

4.3 SOLUTIONS BASED ON VELOCITY-WEAKENING FRICTION

The normalized VW friction law from Equation (3) is $\phi(v)=1-v/\upsilon$ where $\upsilon=V_c/D_0\omega_0$ is the dimensionless characteristic velocity. Equation (6) becomes

$$\partial^2 u/\partial\tau^2=h^2(\partial^2 u/\partial\xi^2)-u-(1-v/\upsilon) \tag{15}$$

When $v>\upsilon$, $\phi(v)$ is negative and unreasonable. Hence, Equation (15) works only for $v<\upsilon$. The LT of Equation (15) is

$$s^2U(\xi,s)=h^2\partial^2U(\xi,s)/\partial\xi^2-U(\xi,s)-1/s+sU(\xi,s)/\upsilon \tag{16}$$

This gives

$$h^2\partial^2U/\partial\xi^2-(s^2+1)-s\upsilon^{-1})U=1/s \tag{17}$$

Let $\zeta=(s^2+1-s\upsilon^{-1})^{1/2}$. The general solution of Equation (17) is

$$U(\xi,s)=C_1e^{-\zeta\xi/h}+C_2e^{-\zeta\xi/h}-1/s\zeta^2 \tag{18}$$

There are two types of waves from Equation (18): the first one is the travelling waves represented by the first term (travelling along the positive direction along the ξ-axis) and second term (travelling along the negative direction along the ξ-axis) in its right-handed-side, i.e., $U_c(\xi,s)=C_1e^{-\zeta\xi/h}+C_2e^{-\zeta\xi/h}$, and the second one is the oscillation at site shown by the third term, i.e., $U_p(\xi,s)=-1/s\zeta^2$. The second term of the first type of waves with $\xi<0$ can be re-written as $e^{-\zeta|\xi|/h}$. The ILT of $U_c(\xi,s)$, i.e., $\mathcal{L}^{-1}[U_c(\xi,s)]$ with $|\xi|/h>0$ is

$$u_c(\xi,\tau)=C\{1-(\sigma|\xi|/h)e_\tau^{/2\upsilon}J_1[\sigma(\tau^2-(|\xi|/h)^2)^{1/2}]/(\tau^2-(|\xi|/h)^2)^{1/2}\}H(\tau-|\xi|/h) \tag{19}$$

where $\sigma=(1-1/4\upsilon^2)^{1/2}$. Because of $\sigma>0$, $1-1/4\upsilon^2$ must be larger than 0 and thus $\upsilon>1/2$. Equation (19) exhibits a travelling plane wave. The quantities inside {...} before $H(\tau-|\xi|/h)$ denote the wave amplitude. Unlike Equation (9) for SW friction, this equation has an extra term $e^{\tau/2\upsilon}$, which increases exponentially with time. When the wave propagates from 0 to ξ_L, the normalized duration time is $\tau_D=\xi_L/h$ and thus the duration time is $T_D=\tau_D/\omega_0=\xi_L/\omega_0h=(L/D_0)/\omega_0h$. Let t_r be the arrival time when the rupture arrives at a site y, that is, $t_r=|y|/v_R$. Substituting $u_c(\xi,\tau)=x_c(y,t)/D_0$, $\xi=y/D_0$, $\tau=\omega_0t$, $t_r=|y|/v_R$, and $\varpi=\omega_0/2\upsilon$ into Equation (19) leads to

$$x_c(x,t)=CD_o\{1-(\sigma\omega_0t_r)e^{\varpi t}J_1[\sigma\omega_0(t^2-t_r^2)^{1/2}]/(t^2-t_r^2)^{1/2}\}H[\omega_0(t-t_r)] \tag{20}$$

When $\varpi<<1$ Hz, $e^{\varpi t}\approx1$ makes Equation (20) be similar to Equation (9). The results are similar to those for SW friction as mentioned above. This condition is equivalent to $\omega_0<<1$ *Hz* or $\upsilon>>1$. Since the wave with $\omega_0<<1$ Hz is a very long wave, it cannot be a slip pulse. When ϖ is not a small value, we examine the properties of $x_c(x,t)$ by using the function $S_v(y,t)=1-(\sigma\omega_0t_r)e^{\varpi t}J_1[\sigma\omega_0(t^2-t_r^2)^{1/2}]/(t^2-t_r^2)^{1/2}$. Define θ to be $\sigma\omega_0(t^2-t_r^2)^{1/2}$. $S_v(y,t)$ can be represented by $1-(\sigma^2\omega_0^2t_r)e^{\varpi t}J_1(\theta)/\theta$. When $t=t_r$, θ=0 and $J_1(\theta)=0$. This leads to an indefinite value of $J_1(\theta)/\theta$. Like the above-mentioned mathematical manipulation for SW friction, we have $lim_{\theta\to0}[J_1(\theta)/\theta]=1/2$. Hence, $x_c(y,0)=CD_0/2$ and $C=2x_c(y,0)/D_0$. As mentioned above, the value of constant C depends on the initial value of $x_c(y,0)$ and thus C must be in general small. The function $J_1(\theta)$ is positive, but vibrates and decreases with increasing θ, and $(t^2-t_r^2)^{-1/2}$ or θ^{-1} also decays fast with time when $t>t_r$.

The value of T_R of a slip pulse at a site is measured from the arrival time, t_r, at a site to the time, t^*, when the amplitude of slip pulse reaches its peak value. This gives $T_R=t^*-t_r$. To obtain t^*, we must calculate the time when $S_v(y,t)$ reaches its peak value from the necessary condition: $dS_v(y,t)/d_t=0$. This can be obtained by taking $dS_v(y,t)/d_t=[dS_v(\theta)/d\theta]d\theta/dt=0$. Since $d\theta/dt=t(t^2-t_r^2)^{-1/2}$ cannot be zero when $t>0$, we only need to consider if $dS_s(\theta)/d\theta$ equals zero. Mathematical manipulation leads to $dS_v(\theta)/d\theta=-(\sigma^2\omega_0^2t_r)e^{\varpi t}\{\varpi J_1(\theta)-[J_0(\theta)-J_1(\theta)/\theta]\}$. From

the rule of Bessel functions that not any two Bessel functions have the same zero, the function $\varpi J_1(\theta)$-$[J_0(\theta)$-$J_1(\theta)/\theta]$ cannot be zero. When $J_1(\theta)=0$ at $\theta=\theta^*$, $J_0(\theta^*)$ is not zero. This results in $\varpi J_1(\theta^*)$-$[J_0(\theta^*)$-$J_1(\theta^*)/\theta^*]$=-$J_0(\theta^*)\neq 0$. When $J_0(\theta)=0$ at $\theta=\theta^*$, $J_1(\theta^*)$ is not zero. This results in $\varpi J_1(\theta^*)$-$[J_0(\theta^*)$-$J_1(\theta^*)/\theta^*]$=$(\varpi+1/\theta^*)J_1(\theta^*)\neq 0$. Meanwhile, $e^{\varpi t}$ is equal to 1 at $t=0$ and larger than 1 when $t>0$. Hence, $dS_v(\theta)/d\theta$ cannot be zero and there is not an extremum for $S_v(y,t)$. This cannot yield $T_R/T_D<0.3$ and thus slip pulses do not exist for VW friction. Unlike $S_s(y,t^*)$, $Sv(y,t)$ does change from positive to negative passing through zero. An example of a normalized waveform $S_v(y,t)/S_{vmax}$, where S_{vmax} is the maximum value of S_v in the figure, of the rupture wave having a propagation velocity of v_R=2 km/sec and the predominant angular frequency of ω_0=1 Hz at a position on the y-axis when the wave propagates with a travelling time t_r=3.607 sec under the action of velocity-weakening friction force with σ=0.9. This plot which shows an increase in the amplitude with time, thus suggesting a crack-like rupture with long T_R. Hence, SV friction can yield pulse-like ruptures only when $\upsilon>>1$ or $V_c>>1$ and in general produces crack-like ruptures.

The third term of Equation (18), i.e., $U_p(\xi,s)$=$-1/s(s^2+1-s\upsilon^{-1})$, is not a function of locality and thus only represents the oscillations at all sites on the fault. But, it is still significant to examine if it behaves like a pulse-like oscillation or not. The function $U_p(\xi,s)$ can be re-written as $-1/s$-$[1-(1-4\upsilon^2)^{1/2}]/2(1-4\upsilon^2)^{1/2}(s-b)$-$[1+(1-\upsilon^2)^{1/2}]/2(1-\upsilon^2)^{1/2}(s-c)$, where $b=(1/2\upsilon)[1+(1-4\upsilon^2)^{1/2}]$, and $c=(1/2\upsilon)[1-(1-\upsilon^2)^{1/2}]$. The solution does not exist when $1-4\upsilon^2=0$ or $\upsilon=0.5$. When $1-4\upsilon^2\neq 0$ or $\upsilon\neq 0.5$, $\mathcal{L}^{-1}[U_p(\xi,s)]$ is

$$u_p(\xi,\tau)=-\{1+(e^{\tau/2\upsilon}/\varepsilon)[e^{\tau/2\upsilon}-e^{\tau/2\upsilon}+e^{\tau/2\upsilon})/2] \qquad (21)$$

where $\varepsilon=(1-4\upsilon^2)^{1/2}$. For $u_c(\xi,\tau)$,υ must be larger than 0.5 as mentioned above. Let $q=(4\upsilon^2-1)^{1/2}=i\varepsilon$. Consider a right triangle with three sides: the longest side with a length of $R=(1^2+q^2)^{1/2}=2\upsilon$, and the other two with lengths of q and 1, respectively. The angle between the longest side and the side with $L=1$ unit is set to be θ. Hence, we have $cos(\theta)=1/2\upsilon$, $sin(\theta)=q/2\upsilon$, and $tan(\theta)=q$. The tangent term gives $\theta=tan^{-1}(q)$. Define $sin(q\tau/2\upsilon)=(e^{iq\tau/2\upsilon}-e^{iq\tau/2\upsilon})/2i$ and $cos(q\tau/2\upsilon)=(e^{iq\tau/2\upsilon}+e^{-iq\tau/2\upsilon})/2$. Replacing $u_p(\xi,\tau)$ by $x_p(y,t)/D_0$, ξ by y/D_0, τ by $\omega_0 t$, and $\varpi=\omega_0/2\upsilon$ into Equation (21) leads to

$$x_p(y,t)=-D_o[1+e^{\varpi t}sin(q\varpi t-\theta)/\sin(\theta)] \qquad (22)$$

Obviously, the initial value of $x_p(y,t)$ is 0 when $t=0$. This $x_p(y,t)$ shows a sine-function-type oscillation at a site. Unlike Equation (14), this equation has an extra term $e^{\varpi t}$, which increases with time. When $t\leq 0$, $x_p(y,t)$ is zero and thus Equation (22) becomes $x_p(y,t)H(t)$. Define $\omega^*=q\varpi=(1-1/4\upsilon^2)^{1/2}\omega_0$ and $T_p=2\pi/\omega^*$ to be, respectively, the predominant angular frequency and the predominant period of the oscillation.

From Equation (22), the particle velocity is $dx_p(y,t)/dt=-D_o\varpi e^{\varpi t}sin(q\varpi t)/cos(\theta)sin(\theta)]$ and the particle acceleration is $d^2x_p(y,t)/dt^2=-D_0\varpi^2e^{\varpi t},sin(q\varpi t,+\theta)/cos^2(\theta)sin(\theta)]$. When $q\varpi t+\theta=\pi$, we have $d^2x_p(y,t)/dt^2=0$. Hence, $\max\{dx_p(y,t)/dt\}=D_0\varpi e^{(\pi-t)/q}$. This holds before the first zero-crossing of dx_p/dt. Hence, the condition of $D_0\varpi e^{(\pi-t)/q}<V_c$, which gives $\upsilon=1.744$, is required.

The plot of T_o/T_p versus υ is displayed in Figure 7b. Clearly, increasing rate of T_o/T_p with υ is high when $\upsilon<1.744$ and becomes low when $\upsilon>1.744$. Although T_p is determined by T_0 ($0.1<T_0<10$) here, the value of T_0 for natural faults is not exactly determined. T_0 is defined by the stiffness of a leaf spring and the mass of the slider. As widely known, natural fault systems are usually self-similar, so that the unique characteristic period of faulting is T_D. Even if natural faults show pulse-like behaviour, their own T_p is not necessarily related to T_0. Elbanna and Heaton [2012] claimed that simultaneous movement of only 10 to 20 sliders in a spring-slider system consisting of 5000 sliders lead to a slip pulse.

From Figure 8, $T_p/T_D=(1-1/4\upsilon^2)^{-1/2}v_RT_0/L$ is a good indication of the presence of a slip pulse for VW friction. Figure 10 shows the plots of T_p/T_D versus υ: (a) for v_RT_0=0.5, 1.0, 1.5, 2.0, 2.5, 3.0, 3.5, and 4.0 km (from bottom to top) when L=80 km; and (b) for L=20, 40, 60, 80, 100, 120, 160, and 180 km (from top to bottom) when v_RT_0=2.0 km. As mentioned above, the quantitative criterion to confirm the existence of a slip pulse is $T_R/T_D<0.3$. Now, T_R is almost equal to T_p. The upper bound of T_p/T_D in the figure is 0.3. Meanwhile, the solution exists only when $\upsilon>1.744$ (as displayed by a vertical line in the figure). Obviously, the major portion of each curve is below the upper bound, thus suggesting the existence of a pulse-like oscillation in the solution regime.

5. DISCUSSION

The theoretical analyses for the conditions of generating slip pulses are made based on the continuous form of the 1-D BK model in the presence of the linear friction laws: $f(u)=1-u/\Delta$ for SW friction as well as $f(v)=1-v/\upsilon$ for VW friction. The parameters Δ and υ are, respectively, the characteristic distance and the characteristic velocity of the respective law. First, it is neces-

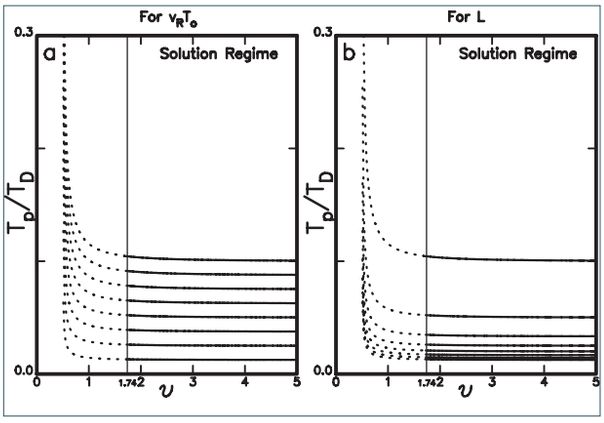

FIGURE 10. The plots of T_p/T_p versus υ: (a) for v_RT_0=0.5, 1.0, 1.5, 2.0, 2.5, 3.0, 3.5, and 4.0 km (from bottom to top) when L=80 km; and (b) for L=20, 40, 60, 80, 100, 120, 160, and 180 km (from top to bottom) when v_RT_0=2.0 km.

sary to consider physical implications of the results. For SW friction, variable transformation of $w=u+\gamma^2$ reduces Equation (7) to the Klein-Gordon equation [Polyanin, 2002]: $\partial^2w/\partial\tau^2=h^2(\partial^2w/\partial\xi^2)-\gamma^2w$. This implies that the strength of the leaf spring has a factor of γ^2 due to presence of friction, so that γ^2 per stored energy within the leaf spring is conserved and $1-\gamma^2$ per the energy is dissipated. We can see that $1-\gamma^2=D_0/X_c$ is a ratio of actual frictional work dissipated due to sliding from an area under SW line in Figure 2a. Since the stiffness of a leaf spring multiplied by γ^{-2} controls energetics, dependence of behavior of the system on k/γ^2 should be discussed.

For VW friction, the restoring force should always have the same sign for stability of the system. Variable transformation of $w=u+1$ reduces Equation (15) to $\partial^2w/\partial\tau^2=h^2(\partial^2w/\partial\xi^2)-w+w'/\upsilon$, where $w'=dw/d\tau$. Without loss of generality, the restoring force can be assumed as negative, i.e., $-w+w'/\upsilon\le0$. Let $F[w]$ be the Fourier transformation of w. Then the following holds: so that should be required, otherwise the friction is not restoring force but repulsive force in high-frequency content. Such a compact supported spectrum in frequency domain is, however, not able to be a compact supported signal in time domain.

There are the complementary solution, $x_c(y,t)$ and particular solution, $x_p(y,t)$, of the equation of motion. For SW friction, the function $x_c(y,t)$ shows a slip pulse when $1>\gamma=(1-\Delta^{-1})^{1/2}>0$. T_R and T_R/T_D both decrease rapidly with increasing t_r, thus meaning that T_R and T_R/T_D are both reduced when the slip pulse propagates along the fault. This means that the slip pulse is generated when the ruptures are far away from the nucleation point. Meanwhile, T_R and T_R/T_D also both decrease when γ, ω_0, and L increase and when v_R is reduced. Higher γ associated with a low decreasing rate of friction with slip is easier to produce a slip pulse than lower γ related to a higher decreasing rate. A decreases in T_R and T_R/T_D with increasing ωo means that slip pulses should have higher angular frequencies and cannot be long-period rupture waves. The decreases in T_R and T_R/T_D with increasing L mean that a slip pulse can be more easily produced in a long fault than in a short one. Hence, it would be difficult to detect a slip pulse on a short fault. Equation (21) shows that lower v_R can more easily result in small T_R and T_R/T_D than higher v_R. This indicates that the slip pulse has a relatively slow propagation speed. However, v_R is less important than other parameters, because the value of v_Rt_r/L in Equation (21) is always smaller than 1.

For VW friction when υ>>1; while it shows a crack-like rupture for VW friction when υ is not too big. The present results suggest that unlike Heaton [1990], SW friction is easier to produce a slip pulse than VW friction. Although Perrin et al. [1995] assumed that not all friction laws result in steady travelling pulses, the present result exhibits that the two types of friction in use can generate a slip pulse under their respective ranges of model parameters.

For the particular solution, the ratio of T_p over T_D of a rupture is a good indication to show the possible existence of a slip pulse, because the T_R of slip at a site is shorter than T_p. For SW friction with Δ>1, the solution clearly shows oscillations with a predominant period of T_p. Computational results in Figure 9 reveal a decrease in T_p/T_D with increasing Δ. Longer (shorter) Δ means a slower (faster) decay of friction with slip. A slower decay of friction with increasing slip is easier to generating a pulse-like oscillation than a faster decay of friction. Based on the definition of $\Delta=X_c>D_0$, Δ>1 gives $X_c>D_0$. This suggests that when the characteristic length is longer than the characteristic distance, the pulse-like oscillation can be generated. Figure 9a shows $T_p/T_D<0.4$ (or $T_R/T_D<0.2$) when Δ>1.2. Figure 9b shows that except for L=20 km, $T_p/T_D<0.4$ (or $T_R/T_D<0.2$) when Δ>1.5. Theoretical results suggest that Δ>1.5 is a significant condition for generating a pulse-like oscillation at a site under SW friction.

For VW friction, when υ>0.5 this solution shows a sine-function oscillation at a site. Because of $\upsilon=V_c/D_0\omega_0$, the inequality υ>0.5 leads to $V_c>D_0\omega_0/2$. This means that a pulse-like oscillation at a site can be generated when $V_c>D_0\omega_0/2$. Since V_c is the characteristic velocity of VW friction law, higher V_c indicates a slower decay of friction with velocity. The present result suggests that a slower decay of friction is more capable of generating the pulse-like oscillation than a

faster one. Unlike the pulse-like oscillation produced by SW friction, the amplitude of pulse-like oscillation generated by VW friction could increase with time due to an extra term $e^{\tau/2\upsilon}$. This suggests that VW friction can cause higher wave energy than SW friction. Smaller υ will cause a faster increase in wave amplitude than larger υ. Figure 10 reveals a decrease in T_p/T_D with increasing υ. Higher (lower) V_c means a slower (faster) decay of friction with velocity. Clearly, a slower decay of friction with velocity is easier to generating a slip pulse than a faster decay of friction. Because of $\upsilon=V_c/D_0\omega_0$, $\upsilon>1$ means $V_c>D_0\omega_0/2$. When the characteristic velocity of the model is higher than the rate of a slider in the characteristic distance, a pulse-like oscillation can be generated. Figure 10 shows $T_R/T_D<0.4$ (or $T_R/T_D<0.2$) when $\upsilon>0.6$. Hence, $\upsilon>0.6$ could be a significant condition for generating a pulse-like oscillation at a site under VW friction.

In addition, Figures 9a and 10a both show a decrease in T_p/T_D with decreasing v_RT_0, which is the characteristic rupture distance. Lower v_R is more capable of generating a pulse-like oscillation than higher v_R. Meanwhile, shorter T_0 is more capable of generating a pulse-like oscillation than longer T_0. Because of $T_0=(m/K_l)^{1/2}/2\pi=(\rho_A/\kappa_l)^{1/2}/2\pi$, strong coupling (denoted by κ_l) between the moving plate and a fault system is capable of producing a pulse-like oscillation than weak coupling. On the other hand, lighter or lower-density fault rocks are easier to producing a pulse-like oscillation than heavier or higher-density fault rocks. Figures 9b and 10b exhibit a decrease in T_p/T_D with increasing L, that is, longer L is more capable of generating a pulse-like oscillation than shorter L. However, the difference in the values of T_p/T_D between two sequential rupture lengths decreases with increasing L. This means that when L is longer than a certain value, the effect of rupture length on T_p/T_D is reduced. Of course, the L-effect also depends on v_R and T_0.

A comparison between Figure 9 and Figure 10 shows that T_p/T_D is in general smaller for VW friction than for SW friction, thus suggesting that the former is more capable of producing a pulse-like oscillation at site than the latter. In addition, under VW friction a pulse-like oscillation can be produced even though L is short.

Based on Equation (7), Wang [2016] obtained that the complementary solution exhibits ω^{-1} scaling in the whole range of ω for SW friction. But, for the particular solution SW friction results in spectral amplitudes only at three values of ω. Based on Equation (15), Wang [2016] obtained that for VW friction with $\upsilon>0.5$, the spectral amplitude versus ω exhibits almost ω_0 scaling when ω is lower than the corner angular frequency, ω_c, which is independent on υ and increases with ω_0. When $\omega>\omega_c$, the spectral amplitude monotonically decreases with ω following a line with a slope value of -1, which is the scaling exponent. This again confirms that crack-like rupture is generated by VW friction. Hence, it is easier to yield slip pulses from SW friction than from VW friction.

6. CONCLUSIONS

Seismological observations show the existence of slip pulses with $T_R/T_D<0.3$. For the present model, there are complementary and particular solutions of the equation of motion. For SW friction, the complementary solution shows a slip pulse when $\gamma>1$. T_R and T_R/T_D both decrease rapidly with increasing t_r, thus meaning that T_R and T_R/T_D both decrease when the slip pulse propagates along the fault. T_R and T_R/T_D also both decrease when γ, ω_0, v_R, and L increase. For VW friction, a slip pulse is yielded when $\upsilon>>1$ or $V_c>>1$ and the crack-like ruptures is generated when υ is not too big. When $\upsilon>>1$ or $V_c>>1$, the results produced by VW friction are essentially similar with those by SW friction. For the two types of friction, a slower decay of friction is more capable of generating slip pulses than a faster one. Lower v_R is more capable of generating a slip pulse than higher v_R. Longer L is more capable of generating slip pulses than shorter L. Of course, the importance of v_R and L are lower than γ and ω_0.

For the particular solution, the ratio of predominant period (T_p) of oscillations at a site is slightly longer than T_R, and thus T_p/T_D, is a good indication to show the existence of pulse-like oscillations at a site because of $T_R<T_p$. Results show the existence of pulse-like oscillations for SW friction when $\Delta>1.6$ (or $X_c>1.6D_0$) and for VW friction when $\upsilon>0.5$ (or $V_c>0.5D_0\omega_0$). T_p/T_D decreases with increasing Δ for SW friction and with increasing υ for VW friction. For the two types of friction, T_0/T_D and T_p/T_D both decreases when v_R and L increase. For the two types of friction, a slower decay of friction is more capable of triggering pulse-like oscillations at a site than a faster one. Shorter T_0 is more capable of generating pulse-like oscillations than longer T_0. In other words, strong coupling between the moving plate and a fault system is capable of producing a slip pulse than weak coupling. Lighter or lower-density fault rocks are easier to producing pulse-like oscillations than heavier or higher-density fault rocks. Longer L is more capable of generating pulse-like oscillations than shorter L.

Acknowledgements. The author would like to thank Prof. A. Bizzarri (Editor of Annals of Geophysics) and an anonymous reviewer for their valuable comments and suggestions to help him to substantially improve this article. This study was financially supported from Academia Sinica, the Ministry of Sciences and Technology (Grant No.: MOST-106-2116-M-001-005), and the Central Weather Bureau (Grant No.: MOTC-CWB-107-E-02).

REFERENCES

Abramowitz, M. and I.A. Stegun (eds.) (1972). Handbook of Mathematical Functions. 9th Edition Dover Publ Inc 1046pp.

Ampuero, J.-P. and Y. Ben-Zion (2008). Cracks, pulses and macroscopic asymmetry of dynamic rupture on a bimaterial interface with velocity-weakening friction. Geophys. J. Int., 173, 674-692 doi:10.1111/j.1365-246X.2008.03736.x.

Ando, R., R. Nakata, and T. Hori (2010). A slip pulse model with fault heterogeneity for low-frequency earthquakes and tremor along plate interfaces. Geophys. Res. Lett., 37, L10310, doi:10.1029/2010GL043056.

Andrews, D.J. (1976). Rupture velocity of plane-strain shear cracks. J. Geophys. Res., 18, 5679-5687.

Andrews, D.J. (1985). Dynamic plane-strain shear rupture with a slip-weakening friction law calculated by a boundary integral method. Bull. Seism. Soc. Am., 75, 1-21.

Andrews, D.J. and Y. Ben-Zion (1996). Wrinkle-like slip pulse on a fault between different materials. J. Geophys. Res., 102, 553-571.

Boatwright, J. (1988). The seismic radiation from composite models of faulting. Bull. Seism. Soc. Am., 78, 489-508.

Beeler, N.M. and T.E. Tullis (1996). Self-healing slip pulses in dynamic rupture models due to velocity-dependent strength. Bull. Seism. Soc. Am., 86, 1130- 1148.

Ben-Zion, Y. and Y. Huang (2002). Dynamic rupture on an interface between a compliant fault zone layer and a stiffer surrounding solid. J. Geophys. Res., 107, B2, 10.1029/2001JB000254.

Beeler, N.M., T.E. Tullis, D.L. Goldsby (2008). Constitutive relationships and physical basis of fault strength due to flash heating. J. Geophys. Res., 113, B01401, doi:10.1029/2007JB004988.

Beroza, G.C. and T. Mikumo (1996). Short slip duration in dynamic rupture in the presence of heterogeneous fault properties. J. Geophys. Res., 101, 22449-22460.

Beroza, G.C. and W.L. Ellsworth (1996). Properties of the seismic nucleation phase. Tectonophys., 261, 209-227.

Biegel, R.L., C.G. Sammis, and A.J. Rosakis (2008). An experimental study of the effect of off-fault damage on the velocity of a slip pulse. J. Geophys. Res., 113, B04302, doi:10.1029/2007JB005234.

Bizzarr, A. (2011). On the deterministic description of earthquakes. Rev. Geophys. 49, RG3002, doi:10.1029/2011RG000356.

Bizzarri. A. and M. Cocco (2006a). Comment on "Earthquake cycles and physical modeling of the process leading up to a large earthquake". Earth Planet Space, 58, 1525-1528.

Burridge, R. and L. Knopoff (1967). Model and theoretical seismicity. Bull. Seism. Soc. Am., 57, 341-371.

Carlson, J.M. (1991). Time intervals between characteristic earthquakes and correlations with smaller events: an analysis based on a mechanical model of a fault. J. Geophys. Res., 96, 4255-4267.

Carlson, J.M. and J.S. Langer (1989a). Properties of earth¬quakes generated by fault dynamics. Phys. Rev. Lett., 62, 632-2635.

Carlson, J.M. and J.S. Langer (1989b). Mechanical model of an earthquake fault. Phys. Rev. A. 40, 6470-6484.

Carlson, J.M., J.S. Langer, B.E. Shaw, and C. Tang (1991). Intrinsic properties of a Burridge-Knopoff model of an earthquake fault. Phys. Rev. A., 44, 884-897.

Cao, T. and K. Aki (1984/85). Seismicity simulation with a mass-spring model and a displacement hardening-softening friction law. Pure Appl. Geophys., 122, 10-24.

Chen, C.C. and J.H. Wang (2010). One-dimensional dynamical modeling of slip pulses. Tectonophys. 487, 100-104.

Chen, K.C., B.S. Huang, W.G. Huang, J.H. Wang, T.M. Chang, R.D. Hwang, H.C. Chiu, and C.C. Tsai (2001). An observation of rupture pulses of the September 20, 1999, Chi-Chi, Taiwan, earthquake from near-field seismograms. Bull. Seism. Soc. Am., 91,1247-1254.

Cochard, A. and R. Madariaga (1996). Complexity of seismicity due to highly rate-dependent friction. J. Geophys. Res., 101, 25321-25336.

Coker, D., G. Lykotrafits, A. Needleman, and A.J. Rosakis (2005). Frictional sliding modes along an interface between identical elastic plates subject to shear impact loading. J. Mech. Phys. Solids, 53, 884-922.

Day, S.M. (1982). Three-dimensional finite difference simulation of fault dynamics: rectangular faults

with fixed rupture velocity. Bull. Seism. Soc. Am., 72, 705- 727.

Da, S.M., G. Yu, and D.J. Wald (1998). Dynamic stress changes during earthquake rupture. Bull. Seism. Soc. Am., 88, 512-522.

Dieterich, J.H. (1972). Time-dependent friction in rocks. J. Geophys. Res., 77, 3690-3697.

Dieterich, J.H. (1979). Modeling of rock friction 1. Experimental results and constitutive equations. J. Geophys. Res., 84, 2161-2168.

Elbanna, A.E. and T.H. Heaton (2012). A new paradigm for simulating pulse-like ruptures: the pulse energy equation. Geophys. J. Int., 189, 1797-1806 doi:10. 1111/j.1365- 246X.2012.05464.x.

Ellsworth, W.L. and G.C. Beroza (1995). Seismic evidence for an earthquake nucleation phase. Science, 268, 851-855.

Ellsworth, W.L. and G.C. Beroza (1998). Observation of the seismic nucleation phase in the Ridgecrest, California, earthquake sequence. Geophys. Res. Lett., 25, 401- 404.

Galetzka, J., D. Melgar, J.F. Genrich, J. Geng, S. Owen, E.Q. Lindsey, X. Xu, Y. Bock, J.-P. Avouac, and L.B. Adhikari (2015). Slip pulse and resonance of the Kathmandu basin during the 2015 Gorkha earthquake, Nepal. Science, 349, 6252, 1091-1095, DOI:10.1126/science.aac6383.

Garagash, D.I. (2012). Seismic and aseismic slip pulses driven by thermal pressurization of pore fluid. J. Geophys. Res., 117, B04314, doi:10.1029/ 2011JB008889.

Heaton, T.H. (1990). Evidence for and implications of self-healing pulses of slip in earthquake rupture. Phys Earth Planet. Int., 64, 1-20.

Huang, W.G., J.H. Wang, B.S. Huang, K.C. Chen, T.M. Chang, R.D. Hwang, H.C. Chiu, and C.C. Tsai (2001). Estimates of source parameters for the Chi-Chi, Taiwan, earthquake, based on Brune's source model. Bull. Seism. Soc. Am., 91, 1190-1198.

Ide, S. and M. Takeo (1997). Determination of constitutive relations of fault slip based on seismic wave analysis. J. Geophys. Res., 102, 27379-27391.

Johnson, E. (1990). On the initiation of unidirectional slip. Geophys. J. Int., 101, 125- 132.

Johnson, R.E. and F.L. Kiokemeister (1968). Calculus with Analytic Geometry. Allyn and Bacon Inc, Boston, Mass, USA, 798pp.

Knopoff, L., J.A. Landoni, and M.S. Abinante (1992). Dynamical model of an earthquake fault with localization. Phys. Rev. A., 46, 7445-7449.

Lapusta, N., J.R. Rice, Y. Ben-Zion, and G. Zheng(2000). Elastodynamic analysis for slow tectonic loading with spontaneous rupture episodes on faults with rate- and state-dependent friction. J. Geophys. Res., 105, 23765-23789.

Lee, S.J., H.W. Chen, and K.F. Ma (2007). Strong ground motion simulation of the 1999 Chi-Chi, Taiwan, earthquake from a realistic 3D source and crustal structure. J. Geophys. Res., 112, B06307, doi:10.1029/2006JB004615.

Lu, X., N. Lapusta, and A.J. Rosakis (2007). Pulse-like and crack-like ruptures in experiments mimicking crustal earthquakes. Proceed. Natl. Acad. Sci., USA, 104, 18931-18936.

Lykotrafits, G., A.J. Rosakis, and G. Ravichandran (2006). Self-healing pulse-like shear ruptures in the laboratory. Science, 313, 1765-1768.

Madariaga, R. and A. Cochard (1994). Seismic source dynamics, heterogeneity and friction. Ann. Geofis., 37(6), 1349-1375.

Marone, C. (1998). Laboratory-derived friction laws and their application to seismic faulting. Annu. Rev. Earth Planet. Sci., 26, 643-696.

Mori, J. and H. Kanamori (1996). Initial rupture of earthquakes in the 1995 Ridgecrest, California sequence, Geophys. Res. Lett., 23, 2437-2440.

Nakayama. W. and M. Takeo (1997). Slip history of the 1994 Sanriku-Haruka-Oki, Japan, earthquake deduced from strong-motion data. Bull. Seism. Soc. Am., 87, 918-931.

Nielsen. S. and R. Madariaga (2003). On the self-healing fracture model. Bull. Seism. Soc. Am., 93, 2375-2388.

Nielsen, S.B. and J.M. Carlson (2000). Rupture pulse characterization: Self-healing, self-Similar, expanding solutions in a continuum model of fault dynamics. Bull. Seism. Soc. Am., 90(6), 1480-1497.

Nielsen, S.B., J.M. Carlson, and K.B. Olsen (2000). Influence of friction and fault geometry on earthquake rupture. J. Geophys. Res., 105, 6069-6088.

Nur, A. (1978). Nonuniform friction as a physical basis for earthquake mechanics. Pure Appl. Geophys., 116, 964-989.

Ohnaka, M. (2003). A constitutive scaling law and a unified comprehension for frictional slip failure, shear fracture of intact rocks, and earthquake rupture. J. Geophys. Res., 108, B2, 2080, doi:10.1029/2000JB000123.

Papageorgiou, A.S. and K. Aki (1983). A specific barrier model for the quantitative description of inhomogeneous faulting and the prediction of strong ground motions. Bull. Seism. Soc. Am., 73, 693-722.

Papoulis, A. (1962). The Fourier Integral and its Applications. McGraw-Hill, 318pp.

Perrin, G., J.R. Rice, and G. Zheng (1995). Self-healing slip pulse on a friction surface. J. Mech. Phys. Solids, 43, 1461-1495.

Polyanin, A.D. (2002). Handbook of Linear Partial Differential Equations for Engineers and Scientists. Chapman & Hall/CRC.

Rice, J.R. (1993). Spatio-temporal complexity of slip on a fault J. Geophys. Res., 98, 9885-9907.

Rice J.R., C.G. Sammis, and R. Parsons (2005). Off-fault second failure induced by a dynamic slip pulse. Bull. Seism. Soc. Am., 95, 109-134.

Ruina, A.L. (1983). Slip instability and state variable friction laws. J. Geophys. Res., 88, 10359-10370.

Shimamoto, T. (1986). Transition between frictional slip and ductile flow for halite shear zones at room temperature. Science, 231, 711-714.

Urata, Y., K. Kuge, and Y. Kase (2008). Heterogeneous rupture on homogenous faults: Three-dimensional spontaneous rupture simulations with thermal pressurization. Geophys. Res. Lett., 35, L21307, doi:10.1029/2008GL035577.

Wald, D.J. and T.H. Heaton (1994). Spatial and temporal distribution of slip for the 1992 Landers, California, earthquake. Bull. Seism. Soc. Am., 84, 668-691.

Wald, D.J., D.V. Helmberger, and T.H. Heaton (1991). Rupture model of the 1989 Loma Prieta earthquake from the inversion of strong-motion and broadband teleseismic data. Bull. Seism. Soc. Am., 81, 1540-1572.

Wang, J.H. (1995). Effect of seismic coupling on the scaling of seismicity. Geophys. J. Int., 121, 475-488.

Wang, J.H. (1996). Velocity-weakening friction as a factor in controlling the frequency-magnitude relation of earthquakes. Bull. Seism. Soc. Am., 86, 701-713.

Wang, J.H. (1997). Effect of frictional healing on the scaling of seismicity. Geophys. Res. Lett., 24, 2527-2530.

Wang, J.H. (2008). One-dimensional dynamical modeling of earthquakes: A review. Terr. Atmos. Ocean. Sci., 19, 183-203.

Wang, J.H. (2009) A numerical study of comparison between two one-state- variable, rate- and state-dependent friction evolution laws. Earthquake Sci., 22, 197-204.

Wang, J.H. (2016). A dynamical study of frictional effect on scaling of earthquake source displacement spectra. Ann. Geophys., 59(2), S0210, doi:10.4401/ag-6974.

Wang, J.H. (2017). Frictional and viscous effects on the nucleation phase of an earthquake nucleation, J. Seismol., 21(6), 1517-1539.

Wang, J.H. and R.D. Hwang (2001). One-dimensional dynamical simulations of slip complexity of earthquake faults. Earth Planets Space, 53, 91-100.

Wu, Z.L. and Y.T. Chen (1998). Solitary wave in a Burridge-Knopoff model with slip- dependent friction as a clue to understanding the mechanism of the self-healing slip pulse in an earthquake rupture process. Nonl. Process Geophys., 5, 121-125.

Zheng. G. and J.R. Rice (1998). Conditions under which velocity-weakening friction allows a self-healing versus a crack-like mode of rupture. Bull. Seism. Soc. Am., 88, 1466-1483.

*CORRESPONDING AUTHOR: Jeen-Hwa WANG,
Institute of Earth Sciences, Academia Sinica,
Nangang, Taipei,
Taiwan

email: jhwang@earth.sinica.edu.tw